Structural and Mechanical Characterization of Poly(Ether Ether Ketone) (PEEK) and Sulfonated PEEK Films: Effects of Thermal History, Sulfonation, and Preparation Conditions

A. Reyna-Valencia, S. Kaliaguine, M. Bousmina

Department of Chemical Engineering (CREPEC), Laval University, Ste-Foy, QC G1K 7P4, Canada

Received 24 November 2004; accepted 17 April 2005
DOI 10.1002/app.22551
Published online in Wiley InterScience (www.interscience.wiley.com).

ABSTRACT: In this work, virgin and sulfonated poly(ether ether ketone) films (PEEK and SPEEK, respectively) have been studied by dynamic mechanical analysis, modulated differential scanning calorimetry, wide-angle X-ray diffraction, birefringence, and optical microscopy. The properties of the unmodified polymer have been addressed to assess the original morphological characteristics and the changes induced by sulfonation. In general, the introduction of ionic groups in the polymer backbone alters dramatically the intrinsic properties of the parent material. The particular thermomechanical response exhibited by PEEK and SPEEK samples, characterized by a hysteresis loop, can be explained by the reversible and irreversible relaxation–orientation of the microstructure, even in the sub-T_g region. The results showed that the preparation conditions largely determine the nonequilibrium morphological features of both compression-molded PEEK films and solvent-cast SPEEK membranes. © 2005 Wiley Periodicals, Inc. J Appl Polym Sci 99: 756–774, 2006

Key words: poly(ether ether ketone) (PEEK); SPEEK; polymer membranes; sulfonation; structure-property relations.

INTRODUCTION

Poly(ether ether ketone) (PEEK) is a semicrystalline thermoplastic polymer that has been extensively studied owing to its several uses as a high-performance material. It has a glass transition temperature of about 143°C, a melting point of ~343°C, and continuous working temperature of approximately 260°C. The high chemical, thermal, and mechanical stabilities of PEEK make it a good candidate as a matrix for composite materials. In addition, chemical modifications of this polymer, specifically sulfonation, are of interest for particular applications. Indeed, PEEK functionalized by electrophilic sulfonation exhibits proton conductivity depending on the degree of sulfonation, while keeping its chemical inertness and thermal stability. These properties make it attractive as a polyelectrolyte material for proton exchange membranes (PEM) for fuel cells.[1–7] However, an increase in the degree of sulfonation, and thus in the proton conductivity, has a negative effect on the mechanical properties, consequently reducing the long-term stability of the material.

This work focuses on the characterization of sulfonated and nonsulfonated PEEK films to evaluate the effects of sulfonation, thermal history, and preparation conditions on their structural and mechanical properties.

The properties of a semicrystalline polymer depend on its thermal history. Therefore, when studying mechanical behavior, changes in the structure as a function of the processing conditions and successive thermal treatments, even at temperatures below the glass transition temperature (T_g), must be taken into account. A number of studies on this subject have been devoted to PEEK. Morphological modifications occurring in PEEK samples during crystallization from the glassy state and in subsequent heating–cooling cycles have been described by several authors. Jonas et al.[8] and Carfagna et al.[9] reported the effect of thermal treatment of amorphous PEEK films below T_g. In general, heat treatment modifies both the amorphous and the crystalline regions to a large extent, and these changes are associated with the metastable character of the glassy structure. These effects are particularly important for PEEK films prepared by compression-molding, as detailed in this work.

Correspondence to: M. Bousmina (bousmina@gch.ulaval.ca).
Contract grant sponsor: CONACyT (Mexico's National Council for Science and Technology).
Contract grant sponsor: NSERC (Natural Sciences and Engineering Research Council of Canada).
Contract grant sponsor: Canada Research Chair in Polymer Physics and Nanomaterials.
Contract grant sponsor: Steacie Fellowship

Furthermore, sulfonation induces important changes in the structure of PEEK, even when the degree of sulfonation is low. The introduction of pendant $-SO_3H$ groups into the polymer alters chain conformation and packing, increases molecular bulkiness, and accordingly causes the loss of the crystalline domains.[10] Moreover, ionic groups interact and modify the intermolecular forces, so hindering segmental mobility.[11] These factors certainly affect the intrinsic properties of the material. For instance, limited chain mobility leads to an upward shift of T_g,[12] while the hydrophilic ionic groups increase moisture affinity and enhance the effect of plasticizers on mechanical behavior.[13]

The preparation method also becomes a key factor in the characterization of the solvent-cast SPEEK membranes, considering the sensitivity of polymer morphology to processing conditions. Polar solvent molecules interact with the polymer ionic groups and are thus very likely to alter membrane morphology during evaporation. In this way, the drying step seems critical for structure development and final mechanical performance.

In the course of this study, the mechanical properties of PEEK and SPEEK films were assessed by dynamic mechanical analysis. Isochronal thermal cycling scans revealed a hysteresis loop in the thermomechanical response related to reversible and irreversible morphological changes induced by thermal treatment in the out-of-equilibrium structure. To address the origin of these observations, structural properties of the films were investigated by the following complementary techniques: modulated differential scanning calorimetry (MDSC), wide angle X-ray diffraction (WAXD), birefringence, and optical microscopy.

This paper consists of two parts. The first deals with the properties of the unmodified PEEK films, which are useful for understanding the structural modifications induced by the introduction of ionic groups. Sulfonation provides the polymer with novel properties and, for this reason, SPEEK membrane characteristics are presented and discussed separately.

EXPERIMENTAL

Membrane preparation

PEEK sheets were pressed from commercial powder (Victrex grade 450P). The dry material was then molded between electrically heated ferrotype platens at 390°C under 10,000 tons for 10 min in a Carver Laboratory hot press. Afterward, air bubbles were removed by compression and release cycles. Cold water was used to cool the platens while maintaining full holding pressure and the mold was removed once the temperature had fallen below 20°C. The films were 100–300 μm thick and only clear and smooth areas were used for the tests. The samples were stored in plastic sealed bags in the laboratory environment and tested within 2 months.

PEEK is sulfonated in the *ortho*-ether position using concentrated sulfuric acid (details on the sulfonation method have been reported elsewhere[6,14]). The degree of sulfonation (DS), i.e., the number of sulfonic groups per polymer repeat unit, can be controlled by reaction time, acid concentration, and temperature. We selected 63%DS and 83%DS samples for this study.

SPEEK membranes were prepared by solvent casting. The dry sulfonated polymer was dissolved (5–10%) in *N*,*N*-dimethylacetamide (DMAc) or dimethylformamide (DMF) and cast onto a glass plate. The membranes were dried at room temperature for 1 day and then gradually heated under vacuum from 25 to 120°C within 8 h and finally kept at 120°C for 2 days.

Sample characterization

Dynamic mechanical analysis (DMA)

Dynamic mechanical analysis was performed in flexural mode using a Rheometrics Solids Analyzer RSAII unit. The selected geometry was the dual-cantilever beam with strips of 45 mm in length and about 5 mm in width. Samples were subjected to isochronal heating and cooling cycles in several temperature ranges above room temperature. Experiments were carried out in air at scanning rates of 0.5, 3, and 18°C/min, and frequencies of 0.1, 1, and 3 Hz.

Conventional and modulated differential scanning calorimetry (DSC and MDSC)

Thermal analysis was performed using a Modulated DSC Q1000 apparatus from TA Instruments in heating and cooling cycles at different rates. The degree of crystallinity of PEEK was calculated by conventional DSC at a heating rate of 20°C/min (130 J/g heat of fusion was assumed for the perfect crystal phase[15]). Samples weighing approximately 7 to 10 mg were tested under nitrogen atmosphere. The temperature and heat-flow were calibrated with pure standards of indium and zinc.

Wide-angle X-ray diffraction (WAXD)

WAXD measurements on pulverized membranes were performed with a Siemens/Bruker X-ray diffraction instrument using copper radiation. The apparatus consists of a Kristalloflex 760 generator, a three-circle goniometer, and a Hi-Star bidimensional detector. The films were reduced to powder using a SPEX Certiprep 5100 Mill. The specimens were immersed in liquid nitrogen and then impact-grounded in a stainless-steel vial set, which was continuously chilled with liquid nitrogen during grinding. The resulting powder was

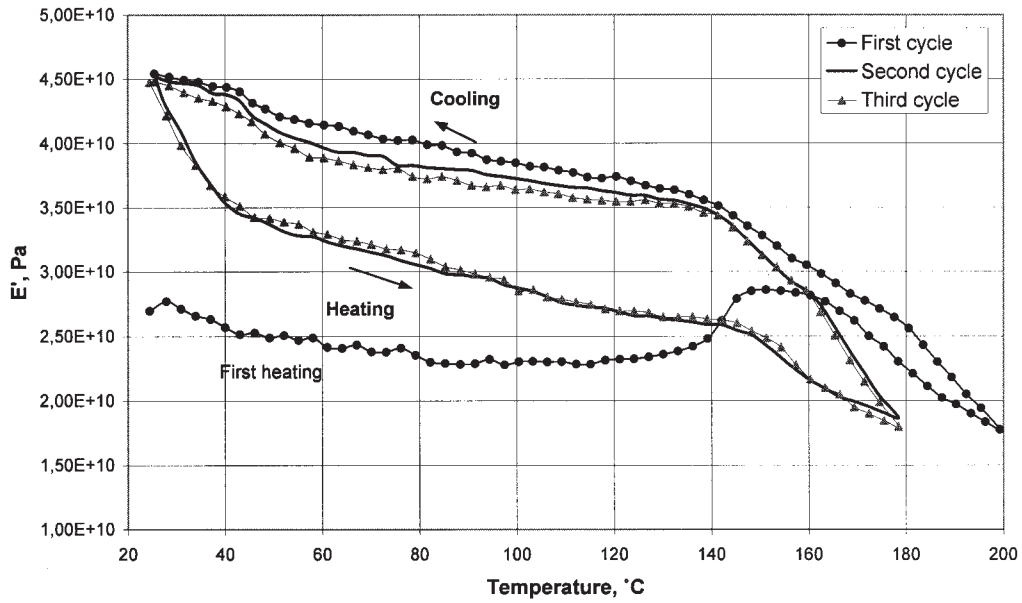

Figure 1 DMA scans of PEEK samples subjected to thermal cycling at 3°C/min.

encapsulated in 1-mm-diameter glass capillaries and analyzed at various temperatures using a heating plate.

Optical microscopy

PEEK morphology was analyzed using a LINKAM THMS 600 hot stage mounted on a Carl Zeiss optical microscope equipped with a digital camera. Small film sections (approximately 10 μm thick) were placed between two 0.16-mm-thick VWR micro cover glasses for observation.

Optical birefringence

Structure orientation in the optically transparent SPEEK samples was detected by birefringence using a Rheometric Scientific ARES instrument equipped with an Optical Analysis Module OAM.

RESULTS AND DISCUSSION

Part I. PEEK film characterization

Dynamic mechanical analysis

With the aim of obtaining insight into the thermomechanical response of the unmodified polymer, untreated PEEK films were subjected to thermal cycling and the evolution of the storage modulus (E') as a function of temperature was monitored during the process. The specimens were heated at 3°C/min to 200°C and then cooled to room temperature with the same rate at a frequency of 0.1 Hz and dynamic deformation of 0.01%.

Data acquired throughout the first scan (Fig. 1) denote that the material response as a function of temperature is strikingly different upon heating and upon cooling. E' values recorded upon cooling are noticeably higher than those obtained during heating. In addition, the heating curve forms a hump in the glass transition region (at 150 $\pm$ ~20°C). Repeating the experiment with the same sample shows that, upon heating, E' values are higher than those observed in the previous heating scan but lower compared to those measured in the cooling process, although they build up again upon cooling. This behavior was reproducible for other samples exposed to similar treatment.

The following points can be drawn from the DMA plots obtained during thermal cycling: the elastic modulus experiences irreversible changes during the first heating process, and, after that, it shows a reproducible hysteresis loop, i.e., the value of E' at a given temperature is lower when it is approached from below (heating the specimen from room temperature) and from above (cooling from high temperature), even if the heating and cooling rates are similar.

Although varying the temperature step during the scans yields essentially the same behavior, the magnitude of the gap between the heating and cooling curves varies with temperature as a function of the heating/cooling rate. As shown in Figure 2, the smaller the temperature step, the greater the distance between the curves. Provided that the heating/cooling rate decreases, the heating curve evidences a downward displacement, whereas the cooling curve shows a further increase as well as a more regular slope.

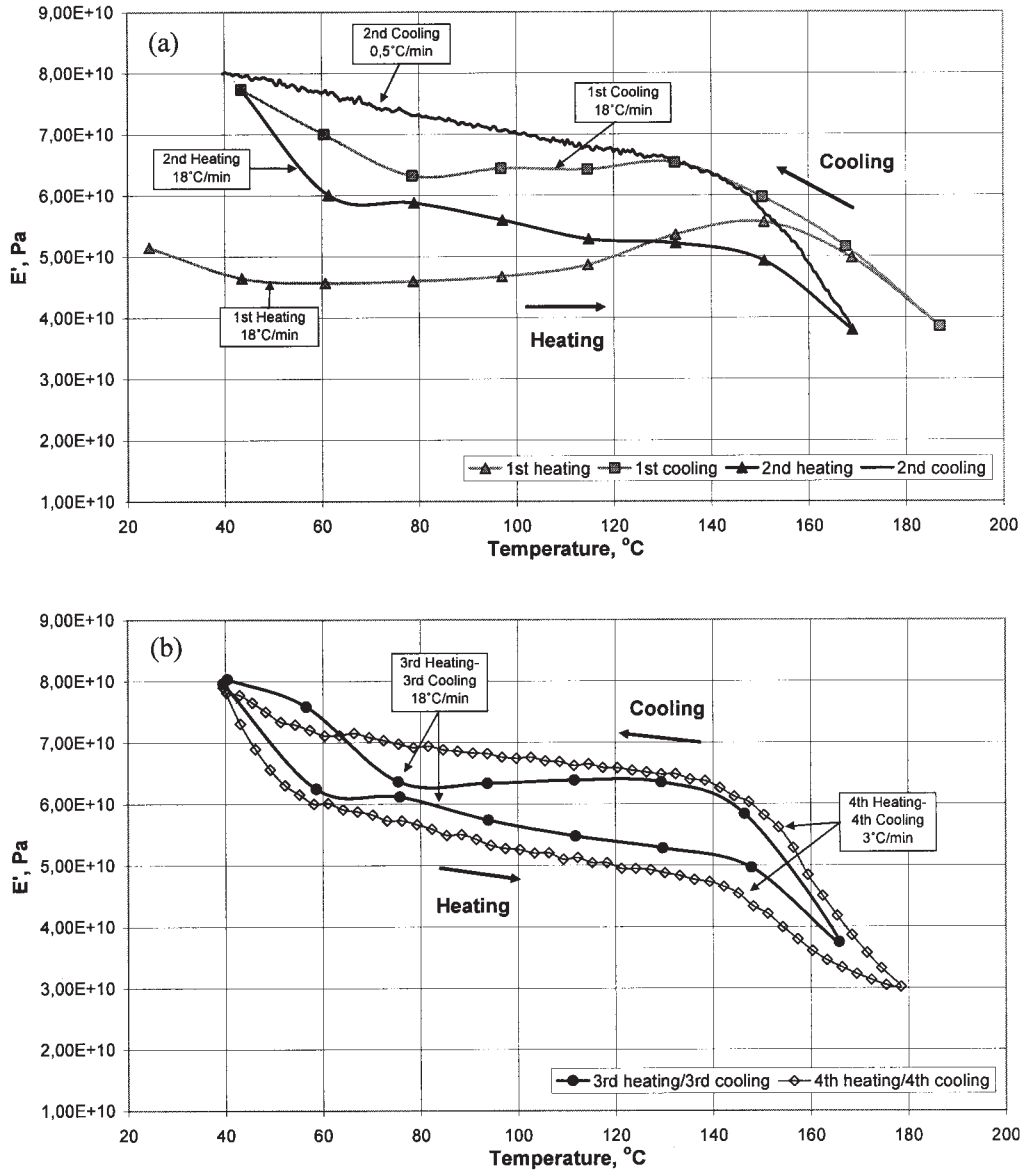

Figure 2 DMA scans of PEEK samples subjected to thermal cycling at various temperature steps (temperature sweeps, frequency fixed at 0.1 Hz, and constant strain of 0.01%): (a) first heating–cooling (18°C/min), second heating (18°C/min), second cooling (5°C/min); (b) third heating–cooling (18°C/min), and fourth heating–cooling (3°C/min).

Thermal cycling performed below the glass transition temperature at various temperature steps produces analogous effects on E' (Fig. 3), suggesting that the material experiences structural changes when submitted to heat treatment below the T_g. The effect of the temperature range was also explored. Figure 4 shows that the gap between the heating and cooling curves decreases when the scans are completed in a smaller temperature range (the thermal history of the specimens subjected to the DMA scans is reported in Table I). Figure 5 illustrates that there is a hysteresis loop even when the difference between the initial and the final temperatures of the scans is very small.

Annealing the sample at 180 or 160°C for several hours during the scans has no apparent effect on the response of the material: The storage modulus of samples subjected to a heating–cooling cycle with no holding time follows the same pathway when submitted to subsequent cycles, including annealing.

It must be emphasized that the highest temperature attained in the first heating cycle is not exceeded to preserve the structure already formed. In fact, the sample loses all memory of the previous treatment by passing over the last temperature reached above T_g.[8] Finally, there is a remarkable mismatch in E' results among specimens.

To sum up, the dynamic mechanical data presented above reveal that heat treatment gives rise to a series of reversible and irreversible thermomechanical transitions in PEEK films. The structural features behind

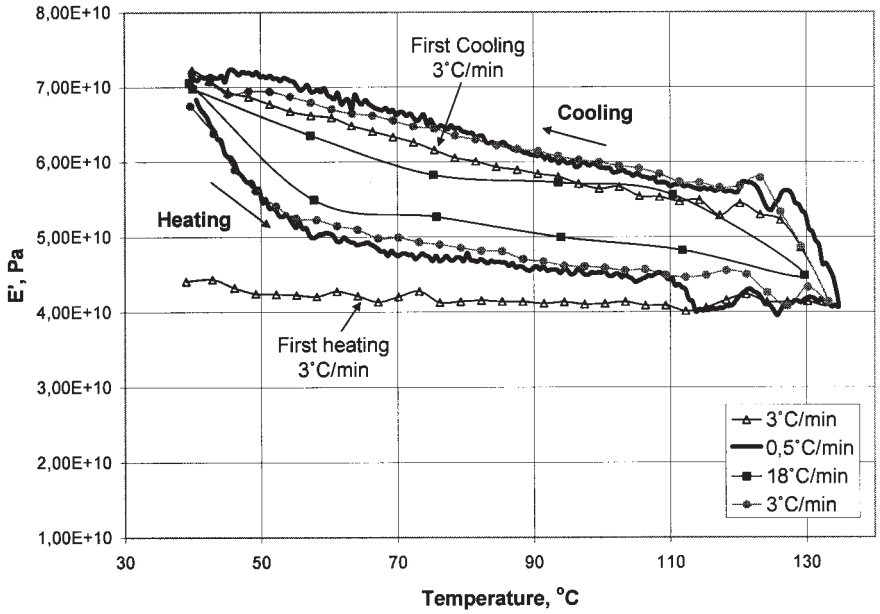

Figure 3 DMA scans of PEEK samples subjected to thermal cycling at various heating/cooling rates below T_g (temperature sweeps, frequency fixed at 0.1 Hz, and constant strain of 0.01%).

these phenomena were further investigated by calorimetry, X-ray analysis, and optical microscopy.

DSC and MDSC

The degree of crystallinity was calculated by conventional DSC for two types of samples: untreated films and specimens exposed to thermal cycles similar to those performed in DMA at 3°C/min (curves are not reported here for the sake of brevity). The difference between the initial crystallinity (27.8%) and that obtained after thermal treatment (28%) was practically insignificant.

Untreated samples were then subjected to thermal cycling and analyzed by MDSC. This extension to conventional DSC provides information about the reversing and nonreversing characteristics of thermal events. Total heat flow comprises two contributions,

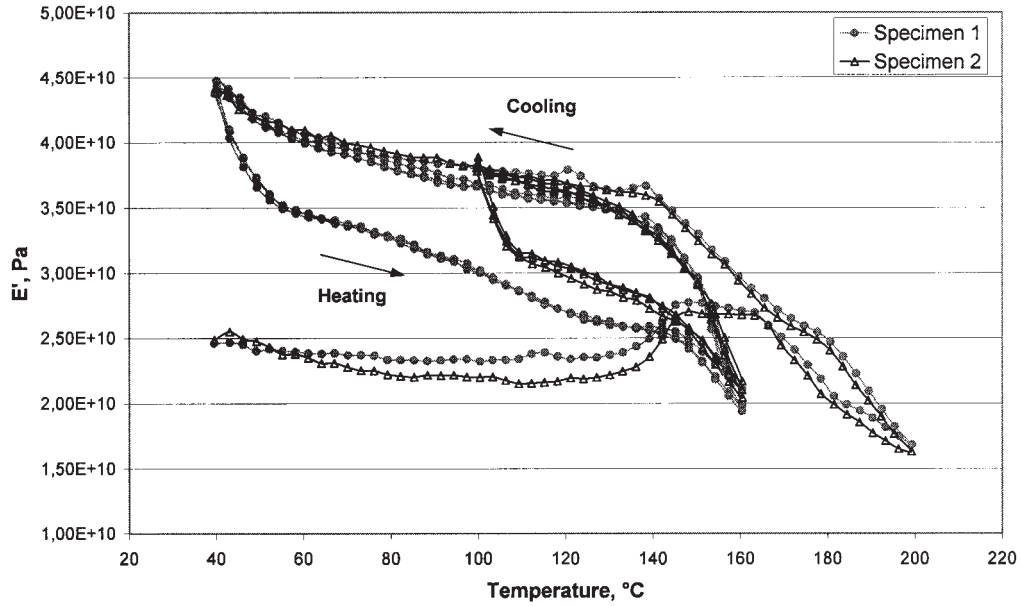

Figure 4 DMA scans of PEEK samples subjected to thermal cycling in different temperature ranges (temperature step: 3 °C/min, frequency: 0.1 Hz, strain: 0.01%).

TABLE I
Thermal History of Specimens Subjected to DMA Scans (Curves Shown in Fig. 4)

	Specimen 1		Specimen 2	
	T_i (°C)	T_f (°C)	T_i (°C)	T_f (°C)
Cycle 1				
Heating	40	200	40	200
Cooling	200	40	200	100
Cycle 2				
Heating	40	160	100	160
Cooling	160	40	160	100
Final cooling			100	40

one of which is heating rate dependent and another, which is dependent only on absolute temperature. Heating-rate-dependent transitions are reversing, i.e., the transition can be cycled by alternating heating and cooling. Absolute temperature-dependent transitions, on the other hand, once initiated, cannot be reversed by thermal cycling.[16]

Figure 6 shows the heating portions of the MDSC scans obtained during thermal cycling at 3°C/min. Each plot consists of three curves, representing reversing heat flow, total heat flow, and nonreversing heat flow. The nonreversing component of the first heating cycle [Fig. 6(a)] evidences that there is an endothermic relaxation during the entire process, from room temperature to above T_g. The curve slightly drives up beyond the T_g region. On the other hand, successive heating cycles [Fig. 6(b,c)] show that there is an endothermic relaxation peak (nonreversing) at the glass transition. These nonreversing events imply the presence of internal molecular stresses, which are relieved on reheating, as well as a rearrangement of the less stable amorphous internal structure.[17] In contrast, there are no appreciable changes in the reversing and total heat flow curves.

The T_g observed in the total heat flow curves shifts to lower temperatures in the thermally treated sample. It goes from 150°C in the first cycle to 147°C in the third one, indicating a less constrained amorphous phase in continuous reorganization.

X-ray analysis

WAXD curves obtained at various temperatures for both untreated films and thermally treated specimens used in DMA exhibit similar characteristics (typical curves are shown in Fig. 7). Diffraction curves collected at room temperature are broad and featureless, resembling the distinctive traces generated by quenched amorphous samples, like those reported in Refs.[15] and [18] Although both films contain about the same degree of crystallinity, as revealed by DSC measurements, the shape of the curves does not suggest the presence of a crystalline phase. The origin of these particular results could be related to the residual stresses of the amorphous domain, which generate nonuniform strains (distortions) in the molecular structure and cause broadening of the diffraction peaks.[19]

In contrast, when the temperature is raised to 150 °C, the corresponding WAXD curves of both films show a small peak at $2\theta = 18.6°$. This slight sharpening could be associated with the processes of struc-

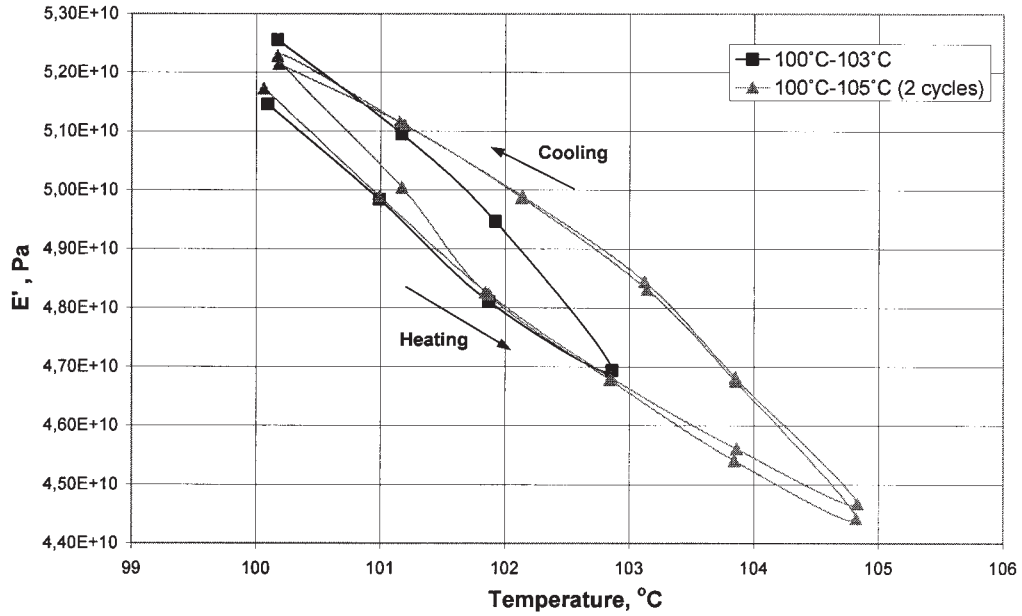

Figure 5 DMA scans of PEEK samples subjected to thermal cycling in a small temperature range (temperature step: 1 °C/min, frequency: 0.1 Hz, strain: 0.01%).

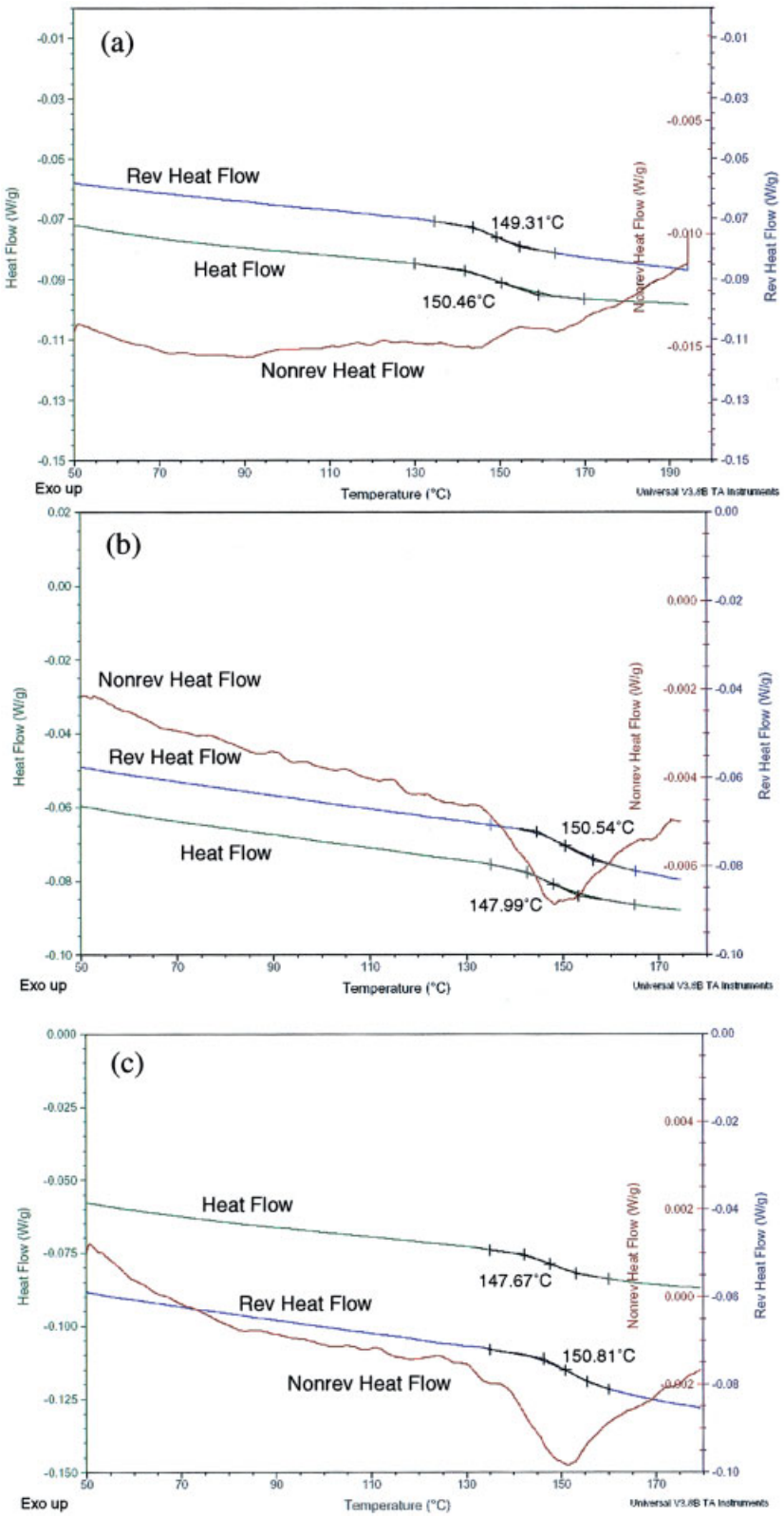

Figure 6 MDSC curves for PEEK films subjected to thermal cycling at 3°C/min: (a) first heating, (b) second heating, (c) third heating.

tural rearrangement and crystallization occurring during thermal treatment. Since the samples are annealed for a short time at low temperature (very close to T_g), cold crystallization is not likely to happen. Instead, this curve profile can be regarded as evidence of internal stress evolution in the semicrystalline samples.

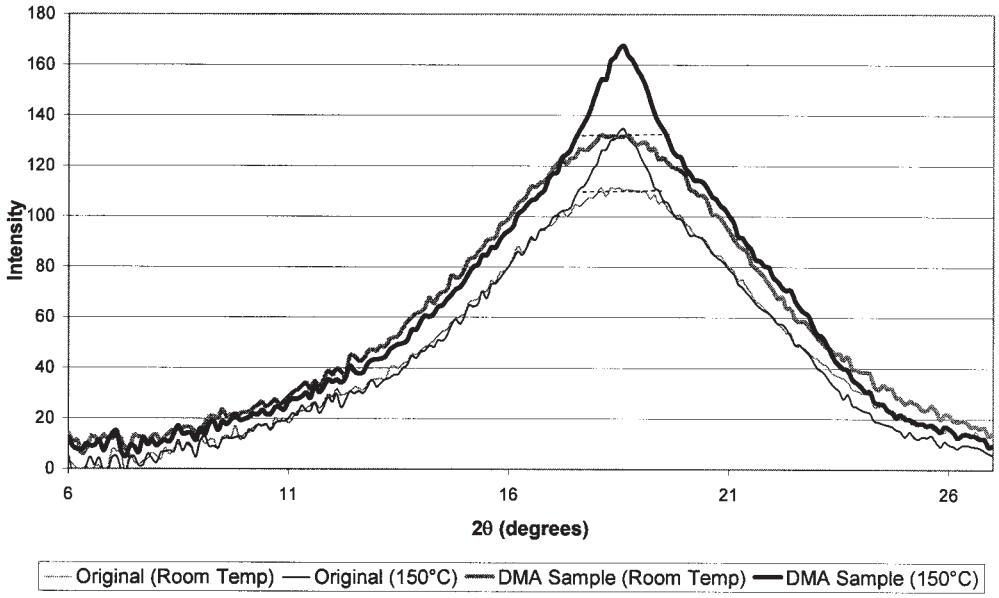

Figure 7 WAXD curves of PEEK samples, obtained at room temperature and at 150°C.

At room temperature, the nonuniform strain due to residual microstresses causes major line broadening, thus hiding the relatively sharp lines that would normally be generated by the crystalline regions. In this way, the only experimentally observable curve at room temperature corresponds to that of an amorphous specimen. Heating brings about relaxation of the mobile amorphous chains, and both macro- and microresidual stresses are reduced in magnitude. As a result, structural rearrangement takes place, tending to orientation and a more organized microstructure, and the broad diffraction lines partially sharpen during annealing.

Curves corresponding to the DMA specimen have slightly greater intensity values. Considering that the testing specimens have approximately the same thickness, this observation might suggest that the amorphous chains get oriented during thermal cycling and part of this molecular orientation remains after cooling.

The shape of the diffraction curves shown in Figure 7 may also reveal the presence of small crystallites in the testing samples (as a general rule, the smaller the crystallites, the wider the diffraction curves). An estimate of the mean crystallite size (L) can be obtained by Scherrer's equation from the width of the diffraction peak:

$$L_{hkl} = \frac{K\lambda}{B \cos \theta}, \qquad (1)$$

where L_{hkl} is the mean dimension of the crystallites perpendicular to the planes (hkl), B is the width at half-tallness of the diffraction peak on the 2θ scale in radians, θ is the diffraction angle, λ is the wavelength of the X-ray, and K is a constant approximately equal to unity and related to the shape of the crystallites assumed to be in the sample.

Numerical calculations for PEEK samples are summarized in Table II. The broken horizontal lines in Figure 9 indicate the portions of the curves that were taken into account for crystallite size determination. In this case, $\lambda = 1.541$ Å and $\theta = 18.6°/2$ (0.16 radian).

Crystallite size values reported in Table II imply the presence of very small crystals. In addition, the value found for a thermally treated specimen is lower than that corresponding to the untreated sample. This apparent unconformity might be due to the use of Scherrer's equation for semicrystalline rather than purely crystalline materials. Indeed, converse to purely crystalline materials, semicrystalline polymers involve nonuniformities in the structure,[20] both at small and at large scales. Under these circumstances, the breadth of the diffraction profile cannot be ascribed exclusively to small crystallite size. Furthermore, since the equation yields a mean value, it might reflect a heterogeneous crystalline structure, the result of skin/core effects generated by different thermal gradients during processing.

TABLE II
PEEK Mean Crystallite Size Calculated by Scherrer's Equation

Sample	B (radian) (Å)	L_{hkl} (Å)
Original (150°C)	0.0157 (0.9°)	99.46
DMA (150°C)	0.0175 (1°)	89.52

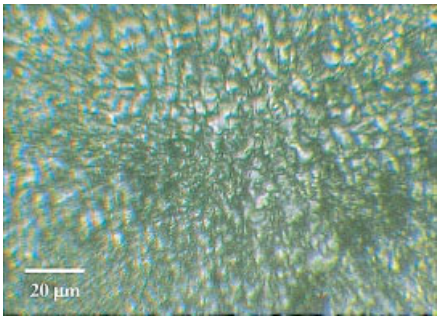

Figure 8 Optical micrograph of a PEEK film at room temperature. [Color figure can be viewed in the online issue, which is available at www.interscience.wiley.com.]

In brief, X-ray analysis makes it evident that internal stresses have pronounced effects on the microstructure and, consequently, on the properties of the studied semicrystalline PEEK films.

Optical microscopy

The morphology of the untreated films was observed under polarized light at room temperature. As illustrated in Figure 8, the micrographs evidence a highly disordered structure consisting of small and imperfect spherulites.

To observe how the morphology changes with temperature and time, the samples were heated to 200°C using a hot stage, kept at that temperature for 12 h, and then cooled to room temperature. The morphological features remained the same, indicating that the evolution of the crystalline phase during the heating–cooling cycles is not significant. Therefore, thermal treatment imparted during this study leaves the crystal fraction practically unaltered, but does affect the amorphous regions of the samples.

Crystallite size estimations from the images obtained by optical microscopy are in clear disagreement with the values found by Scherrer's equation from WAXD curves, with the former results being strikingly higher. The extent of this discrepancy could be due to the sensitivity of the equation to the presence of imperfections in the structure, as explained in the previous section. Another source of variation could be found in the difference of sample thickness used in each case. Samples observed under the microscope were much thinner and this might have had an effect on the final morphology of the specimens, including the crystallite size. Despite this potential dissimilarity in structural features, results issued from this part are useful to verify the evolution of PEEK film morphology.

Overall discussion on PEEK films

The morphology of PEEK films is very sensitive to thermal treatment and yields a very complex thermomechanical response as a consequence of structural reorganization. It is possible to draw a picture of the initial structure of the compression-molded samples. When cooling from the melt, crystallization occurs together with a preceding unmixing, whereby sequences of polymer chains that can be stretched and incorporated into a growing crystal are separated from chain parts near to entanglements, which can only be removed and shifted into the amorphous regions.[21] Cooling is, however, fast and structure formation is governed by kinetic criteria. The structure that develops is that with the maximum growth rather than that with the lowest free energy and, therefore, it has a nonequilibrium character. Crystallites are separated by highly disordered regions and internal stresses accumulate in the amorphous parts of the partially crystalline polymer, as indicated by sample characterization via MDSC and WAXD.

Several studies have shown that the interactions between amorphous and crystalline domains are strong in semicrystalline structures, so the majority of amorphous regions become perturbed, or constrained, upon crystallization. This modification of amorphous regions has been tentatively described in terms of a three-phase model containing a so-called "rigid amorphous phase" (RAP),[22–24] which represents the portion that is constrained and that is different from the liquid-like amorphous fraction. The RAP structure is located at the boundary between the crystals and the mobile amorphous phase and does not undergo a distinctive glass transition; instead, it relaxes gradually as the temperature increases above the T_g of the mobile amorphous phase.[23]

During thermal treatment, when first heated from the glassy state, the chains of the amorphous phase that are constrained between the crystallites absorb energy and then relax. These phenomena would explain the increase in the storage modulus showed by DMA in the T_g region of the first heating curve (Figs. 1, 2, and 4). Once the internal stress has been partially released (a nonreversible event), the amorphous domains gain mobility and the out-of-equilibrium structure reorganizes. Two forces govern this process: the force of rubber elasticity due to the entangled amorphous network tending to pull chains out of the crystal and the thermodynamic driving force toward crystallization.[25] The balance between these mechanisms produces stresses and temperature-dependent changes in the amorphous domains. An input of both thermal energy and thermomechanical solicitation relaxes the chains, thus causing a decrease in E' values, and promotes local orientation toward the interphase region. Alignment of amorphous chains yields higher modulus values in the cooling cycles, having an effect on the mechanical behavior similar to the increase in the degree of crystallinity. During this process, the crystalline domains do not grow significantly, while the liquid-like amorphous phase becomes less constrained, as evi-

denced by the T_g decrease observed in the MDSC curves [Fig. 6(a,b)].

When PEEK is heated from the solid state to above its glass transition temperature, it undergoes cold crystallization from a state of low mobility. Cold crystallization and annealing studies have confirmed the strong influence of the coupling between the lamellae and the noncrystalline regions, revealing that there is a simultaneous evolution of the crystalline and the amorphous domains.[8,26–29] In fact, cold crystallization occurs by a mechanism in which new lamellae progressively fill the free space left between already formed lamellae, and this insertion stops when topological constraints in the interlamellar amorphous regions, such as entanglements, prevent the growth of new lamellae.[8] Ivanov et al.[29] observed that in the low-temperature interval (temperatures below T_g + ~50°C), the slow dynamics of amorphous segments prevents large-scale rearrangements, strongly limiting the process of reorganization. Only lamellar-scale reorganization occurs, resulting in a slight increase of the crystal thickness and perfection. It was also reported that, in this process, the constraints in adjacent amorphous regions increase, as indicated by a T_g raise. In this relaxation-controlled temperature range, the small evolution of the morphological parameters is explained by the blocking mechanism of the slow-moving amorphous interlayers, which preserves the out-of equilibrium state of the reheated semicrystalline structure quite similar to its initial state.

Results issued from the present research are in agreement with the information reported above. Thermal cycling is located in the temperature range addressed by Ivanov et al.[29] and, accordingly, no major changes occur in the crystalline domain. However, the T_g decrease observed in this study indicates that the liquid-like amorphous domains become less constrained after heat treatment. This might suggest that the crystalline zones are relatively isolated by regions of frozen amorphous polymer that limit the interactions between solid and liquid-like amorphous domains. Other studies have demonstrated that no rigid amorphous material relaxes below T_g (except for local and small-scale classical relaxations) and that the material must be exposed to a temperature that overpasses the previous cold-crystallization temperature to show a reduction of the RAP fraction.[23,24] Then, the relaxation phenomena observed in thermal cycling is only due to the mobile amorphous phase, which relaxes and reorients as already described. The boundary created by RAP causes the rigid and liquid-like amorphous phases to reorganize independently during thermal treatment in this particular case.

Time comes into play as a key factor for explaining both the gap variation in the hysteresis loop at different heating/cooling rates and the phenomena observed during thermal cycling in a small temperature range. The slow-moving amorphous chains relax and orient to different extents depending on the time allowed for this phenomenon to occur.

The modulus values obtained experimentally for the films are high compared to typical values of 2–3 GPa reported for PEEK and other semicrystalline polymers in the glassy state, probably because of the great residual stress levels generated by nonisothermal cooling during compression-molding. At high cooling rates, the center of the sample shrinks, introducing further tensile stresses in the core and balancing compressive stresses toward the surface.[30] This means that there are processing-induced strains in addition to individual contributions of the thermal expansion and crystallization shrinkage strains. Therefore, the mechanical response of the semicrystalline material is not uniform through the thickness and the surface of the sample, which might explain the dissimilarities between specimens cut from the same sheet.

This picture of the structural features of the virgin-polymer films is useful to make the distinction between intrinsic and processing-induced properties. The same approach was applied to SPEEK membranes, as described in the second part.

Part II. SPEEK membrane characterization

Dynamic mechanical analysis

Isochronal heat scans were performed at 3°C/min (test frequency 0.1 Hz, dynamic deformation 0.005%) for 63%DS SPEEK samples, conditioned at room temperature and 30% relative humidity. Samples were subjected to three heat–cool cycles, heating from 40°C to above T_g, located at about 180°C as indicated by a peak in the tan δ curve (plots are not reported here), and then cooled to the initial temperature. E' curves (Fig. 9) display essentially the same characteristics as those obtained for PEEK membranes, i.e., the modulus experiences irreversible changes during the first heating process (a drop in this case), followed by a hysteresis loop.

After a large drop in the glass-transition region during the first heating process, E' values rise sharply upon cooling, forming a pronounced step followed by a regular curve with a nearly constant slope. Two regions can also be distinguished in successive heating curves, the first one with practically the same deflection as the cooling curves and the second one with a steeper incline. In the first stage of the cooling processes, E' values are lower than those of the heating curve; then, the modulus builds up and the curves intersect as it continues to rise. The gap between the heating and the cooling curves varies with temperature as a function of their slopes and seems to be different for each testing specimen. T_g values, indi-

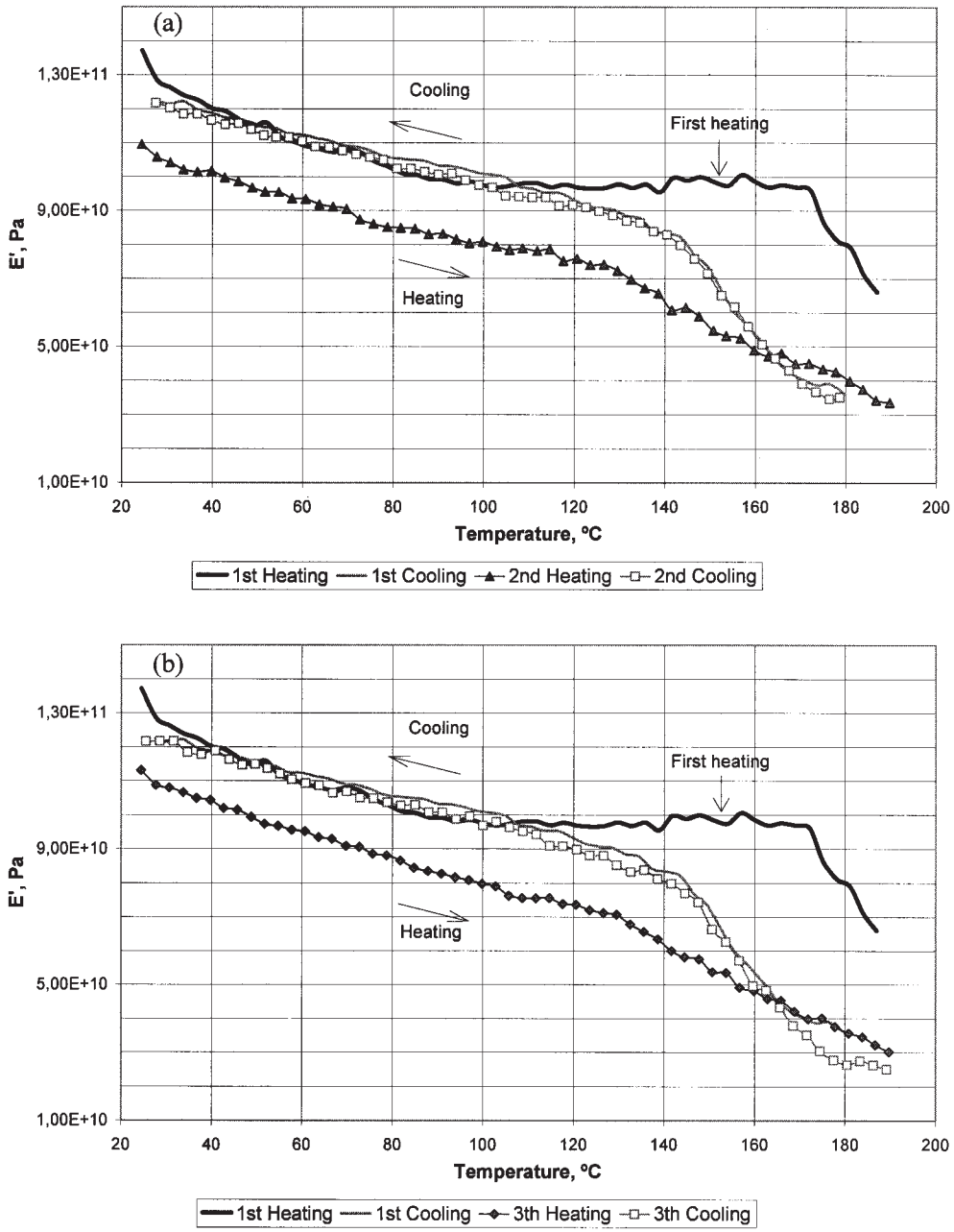

Figure 9 Dynamic elastic modulus of a 63%DS SPEEK sample subjected to three thermal cycles at 3°C/min: (a) first and second cycles, (b) first and third cycles.

cated by the tan δ maxima, evolve as a result of the thermal treatment, as evidenced by results presented in Table III.

When the experiments were repeated for 83%DS SPEEK specimens (Fig. 10), they exhibited a roughly similar behavior, despite the scattering in the experimental data between specimens.

TABLE III
Effect of Heat Treatment on the Location of tan δ Maximum in Successive Thermal Cycles

	tan δ maximum (°C)		
	Heating process		
Sample	First	Second	Third
63%DS SPEEK	178	190	184
83%DS SPEEK	127	129	129

Note: Data collected at 0.1 Hz.

X-ray analysis and birefringence

Translucent 63%DS and 83%DS membranes were studied by WAXD at room temperature and at 150°C.

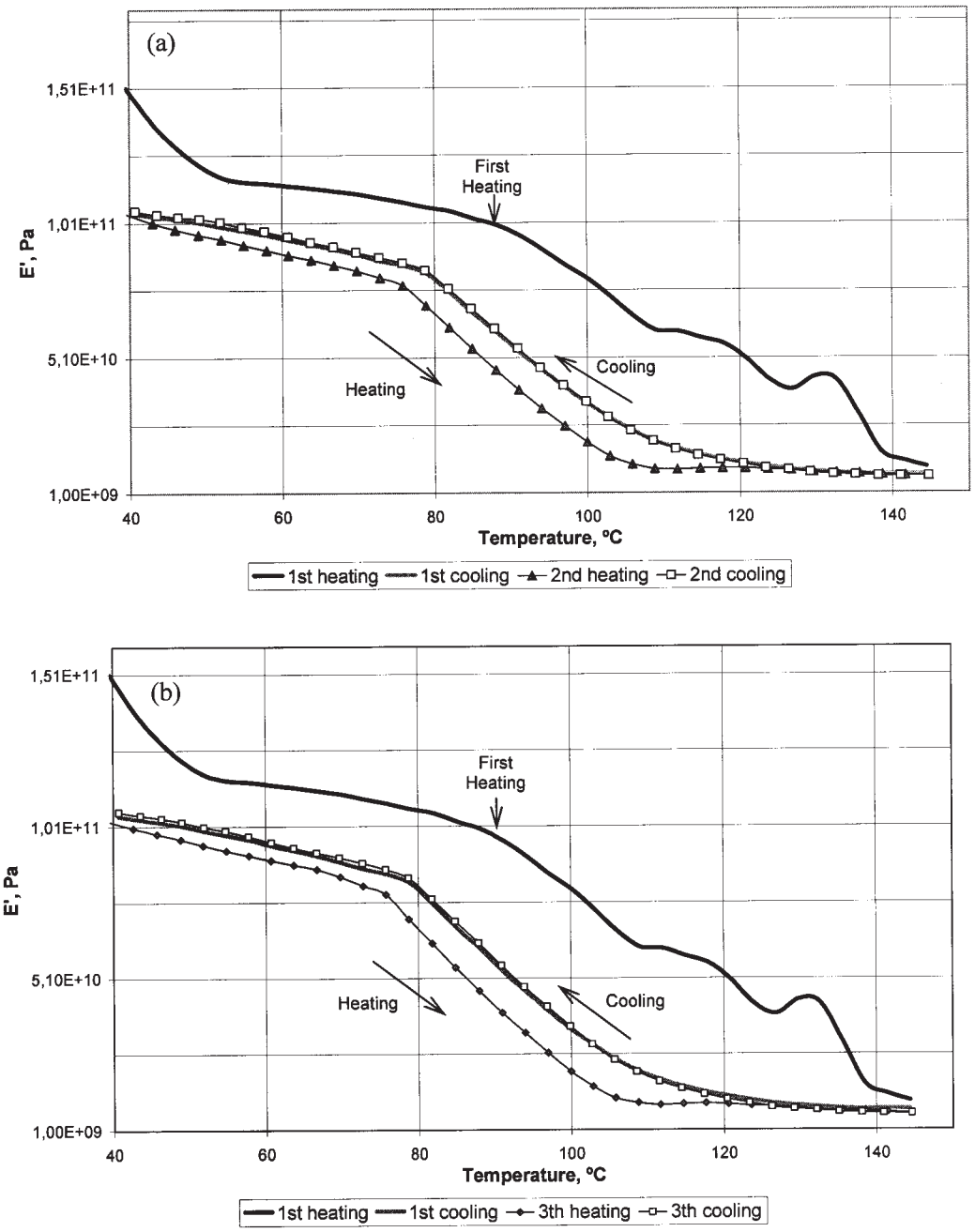

Figure 10 Dynamic elastic modulus of a 83%DS SPEEK sample subjected to three thermal cycles at 3°C/min: (a) first and second cycles, (b) first and third cycles.

Plots of intensity versus diffraction angle 2θ (Fig. 11) corresponding to untreated samples and to specimens used previously in DMA display featureless amorphous curves, suggesting that the polymer contains no crystalline regions. However, these data do not reveal much information about the state of the amorphous structure.

Subsequently, untreated SPEEK films were subjected to thermal cycling and the evolution of their birefringent properties was followed during the process. Data reported in Figure 12 were obtained for a nondeformed 63%DS SPEEK film in a temperature range located in the glassy region. The random positive birefringence values gathered during the first heating scan suggest the relaxation and reorganization of the original structure. In contrast, the subsequent cooling and the second heating–cooling scans yielded higher values that follow regular curves of nearly constant slope, indicating that molecular in-plane orientation was generated during heat treatment.

Amorphous polymers are normally isotropic, yet during sample preparation the molecules may get ori-

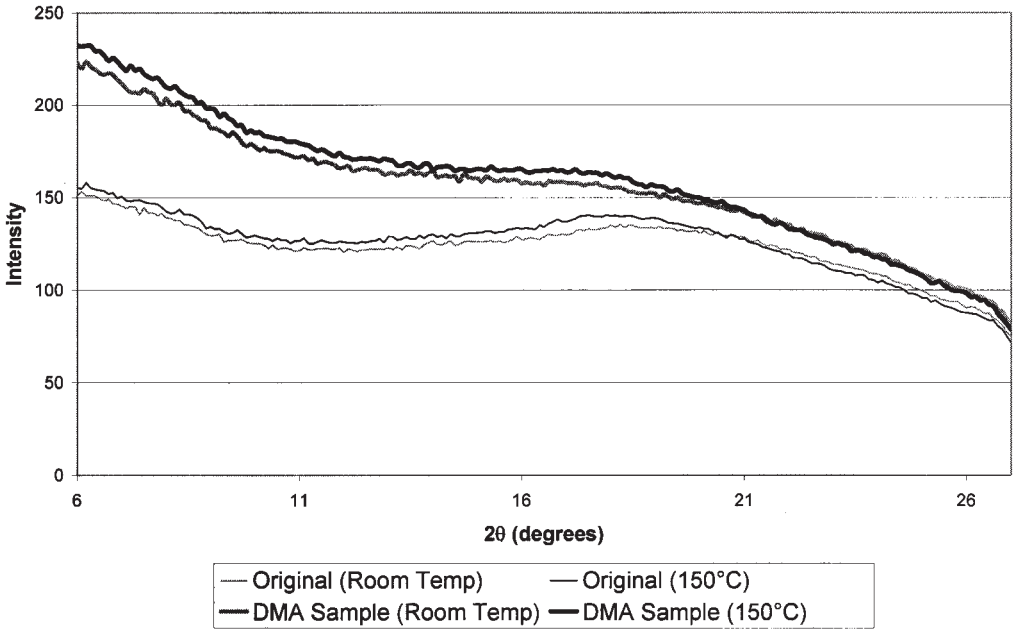

Figure 11 WAXD curves of 63%DS SPEEK samples, obtained at room temperature and at 150°C.

ented due to factors such as viscous flow and solvent evaporation in the case of SPEEK cast membranes. Part of this orientation remains and, in consequence, directional stresses are frozen in the glassy specimen, giving rise to residual stresses. Heat treatment induces relaxation and rearrangement of the mobile chain segments, promoting in-plane orientation in the amorphous structure, as observed in Figure 12. Although this kind of orientation is negligible compared with the directed orientation generated by deforming a polymer at or above its T_g, it does have an effect on the microstructure and, accordingly, on the physical properties.

Since both the refractive index and the stress become anisotropic when a polymer is deformed, the stress–birefringence relationship allows the study of the opticomechanical properties of polymers. For the glassy state, the relation known as photoelasticity stip-

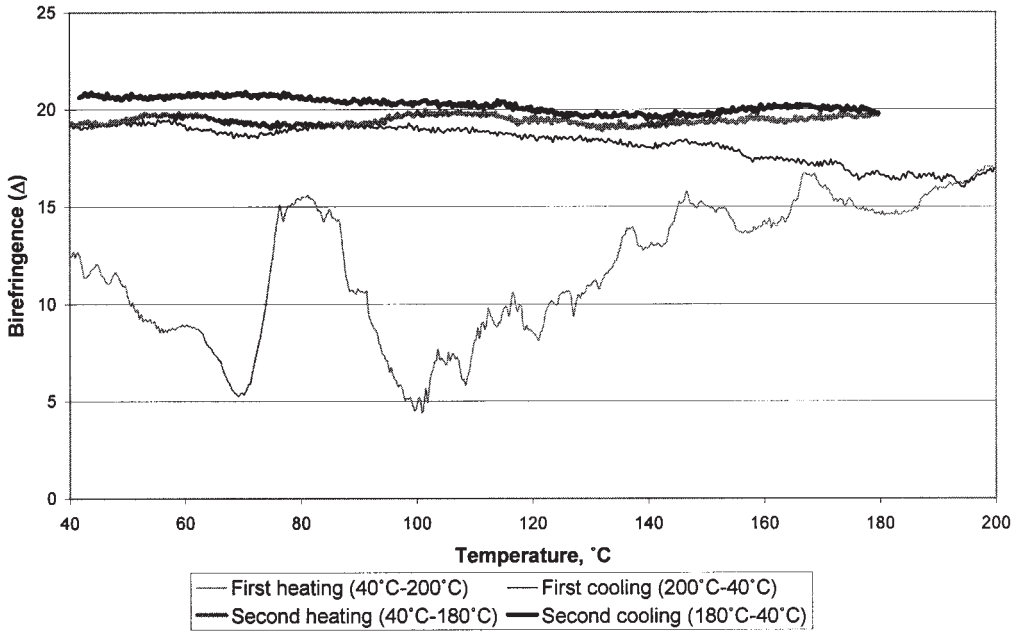

Figure 12 Variation with temperature of the measured birefringence (Δ) of a nonpretreated 63%DS SPEEK specimen subjected to thermal cycling (two heating/cooling cycles, temperature step: 3°C/min).

ulates that the magnitude of the generated birefringence (Δn) is proportional to the difference between the principal stresses present in the structure along and across the optical axis (σ_1 and σ_2), provided that the applied stress is not too large:

$$\Delta n = C(\sigma_1 - \sigma_2). \quad (2)$$

In eq. (2), the proportionality coefficient, C, is known as the stress-optical coefficient. Even if the sample is not stretched, the photoelasticity could be employed to study the state of the oriented amorphous structure resulting from thermal treatment.

With this aim, the value of C for SPEEK below its glass transition temperature should be assessed. In general, the magnitude depends on the chemical structure of the polymer and is rather temperature dependent. Askadskii developed a group contribution method to estimate C for glassy amorphous polymers by means of an empirical equation.[31] However, calculations are cumbersome and this technique yielded unclear results for the SPEEK repeating unit. For this reason, an approximate value was considered satisfactory to obtain only qualitative information about the microstructure of SPEEK specimens. Based on the reported values for other rigid amorphous polymers,[31–33] it was supposed that C for SPEEK is roughly equal to 100×10^{-12} Pa^{-1}.

Using an average value of 20 for the birefringence (taken from Fig. 12), substitution in eq. (2) gives the following outcome:

$$(\sigma_1 - \sigma_2) = \frac{\Delta n}{C} \approx \frac{20}{100 \times 10^{-12}} \approx 2 \times 10^{11} \text{ Pa}.$$

This result provides a general idea of the magnitude of the internal stresses exerted in the oriented amorphous SPEEK specimens following thermal treatment. $\Delta\sigma$ has the same order of magnitude as the E' values observed in DMA near room temperature (Figs. 9 and 10), suggesting that the internal stress and the elastic modulus of the membranes are related somehow.

Finally, it should be mentioned that photoelasticiy is usually defined for an instantaneous response to the stress and does not consider the effect of time. Δn and σ, though, are time-dependent even in the glassy state and, in consequence, the proportionality coefficient C varies over the time range in which the stress changes.[34]

MDSC

The analysis of thermal relaxations exhibited by SPEEK samples was performed by MDSC. As-received membranes were scanned during thermal cycling at 3°C/min and maximum temperature of 180 °C to prevent degradation (it was reported that sulfonic-group decomposition starts at nearly 250°C,[12] but our thermogravimetric tests showed that SPEEK may lose its thermal stability at temperatures close to 200 °C).

Figure 13 shows the results obtained for a 63%DS sample (only the plots corresponding to the first and the second heating scans are shown here, for the sake of brevity). In the first heating, the nonreversing and total heat flow curves exhibited a pronounced endothermic relaxation. In contrast, plots of the subsequent scans show only minor events in the nonreversing curves. The initial large transition can be explained by the relaxation process occurring in the liquid-like amorphous regions that releases the residual stress and facilitates structural reorganization, as confirmed by optical methods. Smaller rearrangements seem to take place in the out-of-equilibrium structure as long as the material is thermally treated.

There are some factors related to polymer synthesis and membrane preparation by solvent-casting that are likely to have an effect on the morphological characteristics of the material. It is expected that solvent molecules modify chain conformation during evaporation from the cast membranes. Moreover, sulfuric acid and organic solvent residues interact with the polymer molecules affecting proton conductivity[35,36] and perhaps the structural properties as well. Washing the membranes with distillate water has been proposed as a solution to this problem,[37] but again diffusing water molecules may alter the morphology of the hydrophilic SPEEK. To assess the contribution of these agents to structure development and evolution during heat treatment, samples of the raw polymer (i.e., that has not been dissolved for casting) along with water-washed membranes were also characterized.

Table IV summarizes the results obtained for 63%DS samples. In general, a pronounced endothermic relaxation is observed in the first heating, but the position of the inversed peak is shifted to higher temperatures in the curves corresponding to the membranes (untreated and washed) by comparison to the raw sulfonated polymer. This fact suggests that residual stress does not result exclusively from membrane manufacture. On the other hand, the upward displacement of the peak might indicate that chains are more constrained in the membranes due to the additional internal stresses generated by solvent evaporation. Washed membranes appear to experience transitions more easily during the first heating and even in later thermal cycling maybe because of the water altered chain-to-chain interactions, facilitating morphologic rearrangements. Traces of sulfuric acid, organic solvent, and water remaining in the structure could act as plasticizers, enhancing the extent of the initial relaxation.

MDSC curves corresponding to 63%DS samples and those of higher %DS samples were similar. In the case

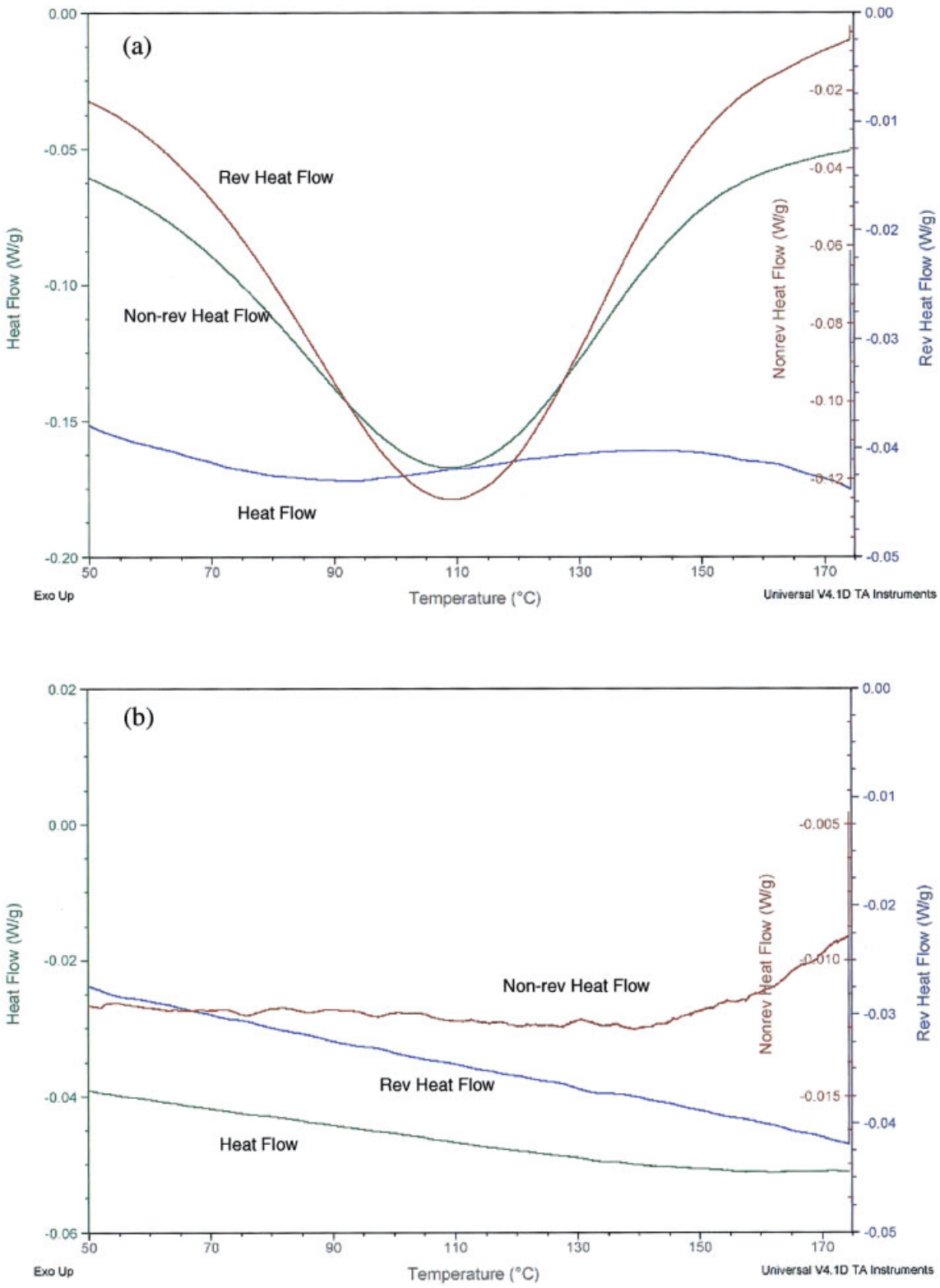

Figure 13 MDSC curves for a 63%DS SPEEK cast membrane subjected to thermal cycling at 3°C/min: (a) first heating, (b) second heating.

of the raw polymer, the main endothermic transition occurred at a slightly higher temperature for the 83%DS sample ($\Delta T \approx 10$°C), probably as a result of the stronger ionic interactions between the molecules. In contrast, the behavior exhibited by both cast-membrane samples was very much alike, as evidenced by

TABLE IV
MDSC Results for 63%DS SPEEK Samples Subjected to Thermal Cycling

Sample	Heating scan	Remarks
Pure polymer	1	Endothermic transition starting at room temperature with minimum located at about 80°C; exhibited by nonreversing and total heat flow curves
	2	Minor unachieved endothermic transition in the nonreversing curve starting at ca. 120°C
	3	Practically featureless
Cast membrane	1	Pronounced endothermic transition starting at room temperature exhibited by nonreversing and total heat flow curves. Minimum located at 110°C (upward displacement of nearly 30°C compared to the pure polymer)
	2	Minor endothermic (nonreversing) event during the entire scan
	3	Minor endothermic (nonreversing) event during the entire scan
Washed membrane	1	Marked endothermic transition starting at room temperature exhibited by nonreversing and total heat flow curves. Minimum located at about 105°C (approximately 25°C above the pure polymer but slightly below the cast membrane)
	2	Small relaxation in the nonreversing heat flow curve (minimum at 150°C)
	3	Small relaxation in the nonreversing heat flow curve (minimum near 140°C)

Figure 14. The tendency shown by these data suggests that there is little difference between the effects produced by both sulfonation levels selected for this study, as if changes stabilize above a critical ionic concentration.

Overall discussion on SPEEK membranes

The results presented above confirm that the ionic nature of sulfonated PEEK strongly influences its morphology and changes the intrinsic properties of the parent polymer. The introduction of sulfonic groups in the polymer backbone as side substituents yields an amorphous structure characterized by stiffer, less mobile chains. Moreover, ionic interactions reinforce the intermolecular forces and undoubtedly affect structural rearrangements, but at the same time ionic groups enhance the plasticizing effects of polar solvents on polymer properties. These microstructural features largely determine their mechanical properties.

Basically, SPEEK is a viscoelastic polymer; therefore, its mechanical response is also sensitive to temperature. In this work, it has been demonstrated that thermal treatment induces molecular reorganization in SPEEK membranes. Experimental evidence suggests that dynamic mechanical properties can be reasonably explained by the structural features resulting from preparation conditions. These films are manufactured by a casting method, where the polymer is dissolved in an organic solvent, namely, DMF or DMAc. During drying, solvent diffusion and evaporation lead to dissimilarities of thickness and molecular structural ordering between contiguous regions of the same film. These factors contribute to the development of residual stresses in polymer films,[32] which can only be released by heat treatment.

In the same way, the solvent remaining in the films undoubtedly influences their mechanical performance, acting as a plasticizer and causing property gradients throughout the samples, thus affecting their morphological structure.[38] It is very likely that its removal from the cast membrane is not complete. In the drying process, solvent evaporation decreases the segmental mobility of polymer chains, and thus the T_g of the polymer/solvent mixture increases. While the film solidifies, it passes from a rubbery material with large diffusion coefficients to a glassy material with much smaller diffusion coefficients; therefore, desorption becomes much slower and some residual solvent is expected to get occluded in the inner part of the samples, as was observed for the evaporation of organic solvents from PEEK.[39,40]

The intrinsic stress caused by constraints on molecular movement due to preparation conditions freezes the polymer chains in a nonequilibrium state. Then, the modulus drop that occurs after the first thermal cycle (Figs. 9 and 10) could be associated with the partial release of the said internal stress, thus reducing the brittleness of the membrane.

This is confirmed by the optical birefringence technique, considering that the degree of in-plane chain orientation in films is sensitive to residual stress, in such a way that random orientation rather than in the film plane generates high residual stresses.[41] Birefringence measurements showed that in SPEEK samples subjected to heat treatment the amorphous chains tend to align themselves in the in-plane direction, implying that the initial residual stress is relieved at some extent and that polymer chains gain mobility to

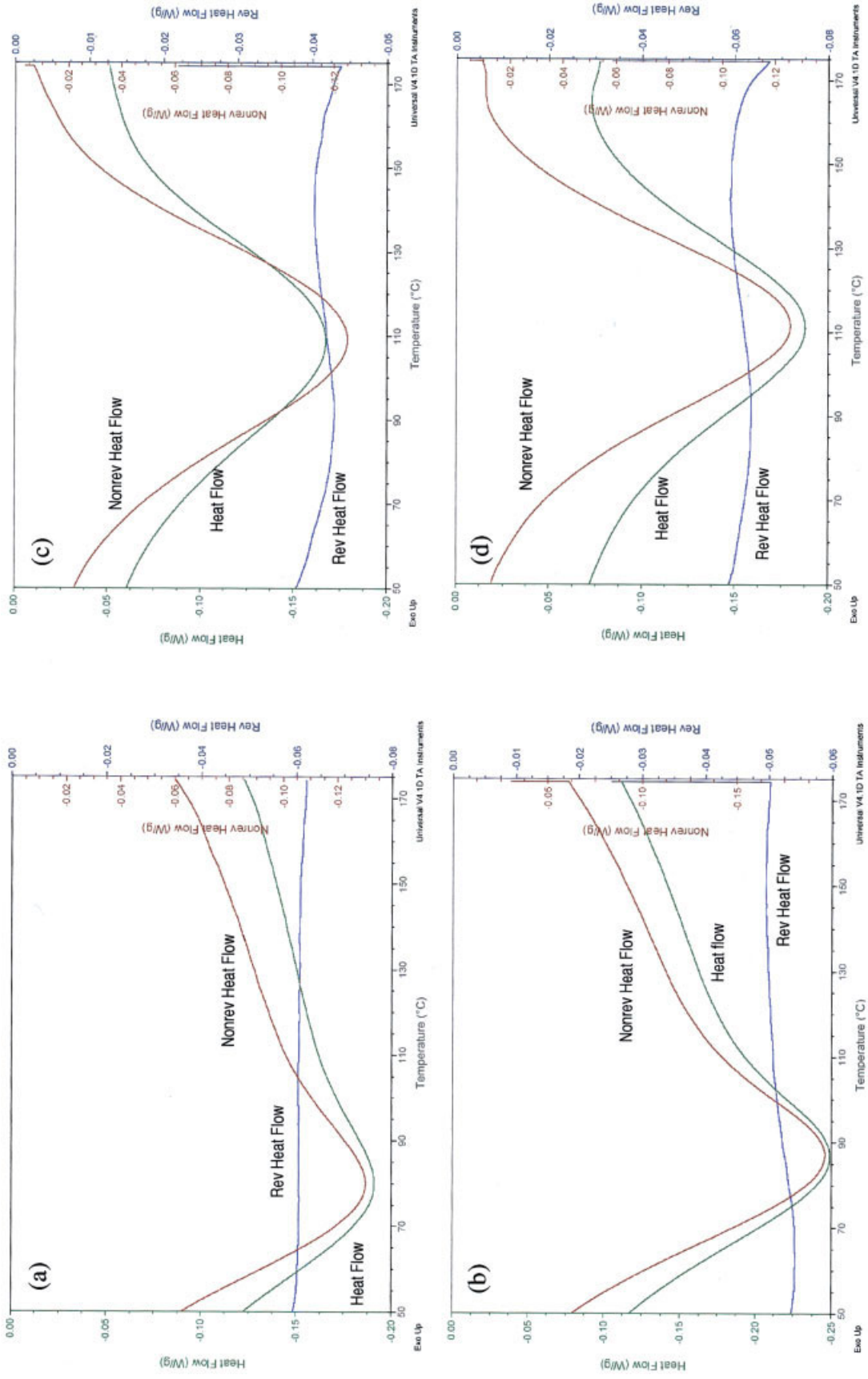

Figure 14 MDSC scans for SPEEK samples subjected to thermal cycling (only the first heating is shown here): (a) 63%DS raw polymer, (b) 83%DS raw polymer, (c) 63%DS cast membrane, (d) 83%DS cast membrane.

rearrange. This observation was verified by MDSC. Moreover, in-plane molecular orientation generated upon thermal treatment increases the T_g of the film. Thus, the relaxation–orientation phenomena are thought to be at the origin of the hysteresis loop in E' plots upon heat–cool cycles. This effect may be enhanced by the presence of occluded solvent in the inner part of the samples, which acts as a plasticizing agent that facilitates rearrangements and orientation during thermal treatment.

The mismatching T_g values between SPEEK specimens suggest yet again the influence of the preparation method. Actually, results obtained by DMA for 63 and 83%DS samples are lower than those reported by Xing et al.,[12] for example. The T_g is expected to increase with higher ionic contents, but results presented in Table III show the reverse behavior. Therefore, in this case the T_g is a very complex function of the composition and the preparation conditions of the membranes.

Another factor that must be taken into account in this discussion is the ionic nature of the polymer. Ionic groups tend to aggregate as a result of electrostatic interactions, despite the opposing tendency of chain elastic forces, to form ion-rich regions in the polymer matrix.[11] This phase separation is promoted by thermal treatment and hence the ionic aggregation process might also have an effect on the dynamic mechanical response of the polymer. The specific effects of ionic interactions were not addressed in this study; however, it was observed that structural reorganization detected by MDSC was very similar for samples with two different sulfonation levels (63 and 83%DS).

In fact, thermally induced morphological changes of SPEEK membranes have been found to affect membrane conductivity.[42] Samples submitted to a sequence of heating-cooling cycles between 100 and 160 °C yielded higher conductivity values after the first heating process, and this improvement was ascribed to irreversible microstructural modifications that favor proton conduction.

In conclusion, sulfonation provides novel morphological properties to PEEK and, as a result, the virgin and the sulfonated polymers display different mechanical responses. Structural rearrangements reflected by changes in the elastic modulus of both PEEK and SPEEK samples cannot be explained by the same mechanisms. Moreover, scattering in experimental results caused by the preparation conditions makes direct comparison impractical.

GENERAL CONCLUSIONS

Semicrystalline PEEK and amorphous SPEEK membranes subjected to heating–cooling cycling experienced morphological changes that generated a reproducible hysteresis loop in E' curves. Characterization performed by different complementary techniques evidenced that this relaxation–orientation behavior results from the reorganization of mobile amorphous chains as a function of temperature, occurring even in the sub-T_g region.

This work on the structure–property relations of PEEK and SPEEK films is important for the assessment of SPEEK as a candidate for PEM fuel cells. Information about the complex structural and mechanical properties of SPEEK membranes resulting from sulfonation, preparation method, and thermal treatment is critical for optimizing their final performance in fuel cells. At the same time, this study highlights the need for further investigation on the development and evolution of microstructural features that result from preparation conditions of PEMs.

Thanks are due to Dr. Serguei Mikhailenko and M.Sc. Keping Wang for their help in sample preparation, as well as to Steve Pouliot for his assistance during the experimental work.

References

1. Kobayashi, T.; Rikukawa, M.; Sanui, K.; Ogata, N. Solid State Ionics 1998, 106, 219.
2. Cui, W.; Kerres, J.; Eigenberger, G. Separ Purif Technol 1998, 14, 145.
3. Rikukawa, M.; Sanui, K.; Prog Polym Sci 2000, 24, 1463.
4. Bonnet, B.; Jones, D. J.; Roziere, J.; Tchicaya, L.; Alberti, G.; Casciola, M.; Massinelli, L.; Bauer, B.; Peraio, A.; Ramunni, E. J N Mater Electrochem Syst 2000, 3, 87.
5. Ise, M.; Kreuer, K. D.; Maier, J Solid State Ionics 1999, 125, 213.
6. Zaidi, S. M. J.; Mikhailenko, S. D.; Robertson, G. P.; Guiver, M. D.; Kaliaguine, S. J Membr Sci 2000, 173, 17.
7. Mikhailenko, S. D.; Zaidi, S. M. J.; Kaliaguine, S. Catal Today 2001, 67, 225.
8. Jonas, A. M.; Russell, T. P.; Yoon, D. Y. Macromolecules 1995, 28, 8491.
9. Carfagna, C.; Amendola, E.; D'Amore, A.; Nicolais, L. Polym Eng Sci 1988, 28, 1203.
10. Jin, X.; Bishop, M. T.; Ellis, T. S.; Karasz, F. E. Br Polym J 1985, 17, 4.
11. Hara, M.; Sauer, J. A. Rev Macromol Chem Phys 1994, C34, 325.
12. Xing, P.; Robertson, G. P.; Guiver, M. D.; Mikhailenko, S. D.; Wang, K.; Kaliaguine, S. J Membr Sci 2004, 229, 95.
13. Reyna-Valencia, A.; Kaliaguine, S.; Bousmina, M.; J Appl Polym Sci 2005, to appear.
14. Wang, K. M. Sc. Thesis: Study of SPEEK-Based Proton Exchange Membranes for Fuel Cell Applications; Laval University: Quebec, 2003.
15. Blundell, D. J.; Osborn, B. N. Polymer 1983, 24, 953.
16. Reading, M. Trends Polym Sci 1993, 1, 248.
17. Gill, P. S.; Sauerbrunn, S. R.; Reading, M. J. Therm Anal 1993, 40, 931.
18. Cebe, P.; Chung, S. Y.; Hong, S. D. J Appl Polym Sci 1987, 33, 487.
19. Cullity, B. D.; Stock, S. R. Elements of X-Ray Diffraction, 3rd ed.; Prentice Hall: Upper Saddle River, NJ, 2001.
20. Alexander, L. E.; X-Ray Diffraction Methods in Polymer Science; Wiley–Interscience: Toronto, 1969.
21. Strobl, G. The Physics of Polymers, 2nd ed.; Springer-Verlag: New York, 1997.

22. Cheng, S. Z. D.; Cao, M. Y.; Wunderlich, B. Macromolecules 1986, 19, 1868.
23. Huo, P.; Cebe, P. Macromolecules 1992, 25, 902.
24. Lu, S. X.; Cebe, P. Polymer 1996, 37, 4857.
25. Mansfield, M. L. Macromolecules 1987, 20, 1384.
26. Ivanov, D. A.; Jonas, A. M. Macromolecules 1998, 31, 4546.
27. Ivanov, D. A.; Jonas, A. M. J Polym Sci B Polym Phys 1998, 36, 919.
28. Ivanov, D. A.; Legras, R.; Jonas, A. M. Macromolecules 1999, 32, 1582.
29. Ivanov, D. A.; Legras, R.; Jonas, A. M. Polymer 2000, 41, 3719.
30. Eduljee, R. F.; Gillespie, J. W. Jr.; McCullough, R. L. Polym Eng Sci 1994, 34, 500.
31. Askadskii, A. A. Physical Properties of Polymers: Prediction and Control; Gordon and Breach: New York, 1996.
32. Bicerano, J Prediction of Polymer Properties, 3rd ed.; Dekker: New York, 2002.
33. Krevelen, D. W.; van; Hoftyzer, P. J. Properties of Polymers, 2nd ed.; Elsevier: Amsterdam, 1976.
34. Inoue, T.; Okamoto, H.; Osaki, K. Macromolecules 1991, 24, 5670.
35. Kaliaguine, S.; Mikhailenko, S. D.; Wang, K. P.; Xing, P.; Robertson, G.; Guiver, M. Catal Today 2003, 82, 213.
36. Robertson, G. P.; Mikhailenko, S. D.; Wang, K.; Xing, P.; Guiver, M. D.; Kaliaguine, S. J. Membr Sci 2003, 219, 113.
37. Mikhailenko, S. D. Personal communication.
38. Park, K. S.; Kwon, Y. D.; Kim, D. Polym J 2001, 33, 503.
39. Arzak, A.; Eguiazábal, J. I.; Nazábal, J. J. Polym Sci B Polym Phys 1994, 32, 325.
40. Wolf, C. J.; Bornmann, J. A.; Grayson, M. J. Polym Sci B Polym Phys 1991, 29, 1533.
41. Ree, M.; Park, Y.-H.; Kim, K.; Kim, S. I. Polymer 1997, 38, 6333.
42. Alberti, G.; Casciola, M.; Massinelli, L.; Bauer, B. J Membr Sci 2001, 185, 73.